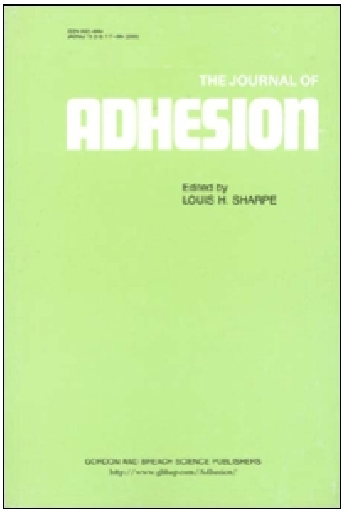

The Journal of Adhesion
Publication details, including instructions for authors and subscription information:
http://www.informaworld.com/smpp/title~content=t713453635

Interphase Composition in Aluminum/Epoxy Adhesive Joints

R. G. Dillingham[a]; F. J. Boerio[a]
[a] Department of Materials Science and Engineering, University of Cincinnati, Cincinnati, Ohio, U.S.A.

To cite this Article Dillingham, R. G. and Boerio, F. J.(1987) 'Interphase Composition in Aluminum/Epoxy Adhesive Joints', The Journal of Adhesion, 24: 2, 315 — 335

To link to this Article: DOI: 10.1080/00218468708075434

URL: http://dx.doi.org/10.1080/00218468708075434

J. Adhesion, 1987, Vol. 24, pp. 315–335

Printed in the United Kingdom

Interphase Composition in Aluminum/Epoxy Adhesive Joints

R. G. DILLINGHAM and F. J. BOERIO

Department of Materials Science and Engineering, University of Cincinnati, Cincinnati, Ohio 45221, U.S.A.

(Received November 10, 1986; in final form July 13, 1987)

Model epoxy/aluminum adhesive joints were constructed with a geometry that allowed cracks to be propagated extremely close to the adhesive/adherend interface. The joints were fractured in air and the fracture surfaces analyzed using angle resolved X-ray photoelectron spectroscopy. Fracture occurred in a manner that left a significant amount of aluminum oxide on the epoxy side of the fracture surface and very little epoxy on the aluminum side. Aliphatic amine curing agent found associated with the aluminum oxide on both the adhesive and the adherend sides of the fracture surface was protonated by the acidic hydroxyls present in the aluminum hydroxide. Moreover, catalysis of the curing reaction by these hydroxyls resulted in an increased degree of crosslinking in the regions of the adhesive very close to the oxide surface. Thus, the aluminum oxide surface modified the structure of the adhesive in the near surface regions and resulted in the formation of a distinct interphase region with a composition different from that of the bulk adhesive.

KEY WORDS Interphases; adhesive joints; X-ray photoelectron spectroscopy; infrared spectroscopy; locus-of-failure; catalysis.

I. INTRODUCTION

The study of the structure and composition of interfaces has led to a much better understanding of the behavior of coatings and adhesives systems. For example, strong adhesive bonds to aluminum have been found to be very dependent on oxide morphology.[1,2] It has been suggested[2] that the single most important factor in obtaining strong adhesive joints is the presence of a microscopically rough oxide surface to permit effective mechanical interlocking between adhesive and substrate.

The chemical composition of an interface can also have a large effect on the strength and durability of an adhesive joint or a coating. For example, during exposure to typical service environments, which generally include moisture, diffusion of water into the interfacial region can result in corrosion of a metallic substrate and subsequent debonding. Alteration of the chemistry of the substrate surface can prevent or greatly retard the occurrence of these corrosion processes. This can be accomplished through chemical conversion of the surface in a process such as anodization[3] or by the adsorption of as little as a monomolecular layer of a corrosion inhibitor.[1,3]

Many investigations of adhesion phenomena have focussed on the structure and properties of interfaces. Much less has been accomplished in determining the manner in which the structure and properties of an organic polymer are altered by curing in contact with the substrate surface. The region of the polymer whose structure and/or chemistry has been influenced by the presence of an interface may extend many molecular layers into the organic phase and has been referred to as the interphase region[4,5] to distinguish it from either bulk phase or interface.

Several previous investigations have demonstrated the presence of an interphase region with different chemical composition from the bulk material. In an analysis of polyimide-SiO_2 adhesive joints tested in peel,[6] X-ray photoelectron spectroscopy (XPS) was used to show that failure occurred close to the interface. The adhesive fracture surface was lacking a nitrogen-containing component that was characteristic of both the bulk adhesive and the substrate side of the fracture surface. This may have been due to the diffusion to the substrate surface of an isoimide component of the adhesive. If this diffusion occurred, it could have created a region devoid of this material near the interface that was mechanically weak. The nitrogen material present on the substrate fracture surface but absent from the adhesive fracture surface may also have been a component of the adhesive that degraded during cure.

Another investigation using XPS to analyze the fracture surface of a nylon/fluorocarbon adhesive joint found that failure occurred in a weak boundary layer near the interface.[7] This region contained the same elements as the constituents of the joint, but showed a stoichiometry different from either the nylon or the fluorocarbon. It was suggested that this was the result of the migration of impurities from the bulk to the interfacial region during manufacture which created a region more susceptible to failure than either of the bulk phases.

Other investigators have demonstrated the formation of interphases that consisted of a region of adhesive with different morphology than the bulk resin. One study used transmission electron microscopy to study nodule formation in epoxy resins cured against various inorganic substrates.[8] In general, small nodules (*ca.* 100 A) were associated with resins cured in close proximity to high energy surfaces (*e.g.*, glass microspheres and copper wires) as well as resin cured with an excess of catalyst. Larger nodules (*ca.* 400–500 A), on the other hand, were associated with resin cured in the absence of interfaces (*e.g.*, bulk specimens) or with resin cured with less than the stoichiometric amount of curing agent. It was suggested that the high energy surfaces were able to adsorb curing agent from the bulk resin which resulted in the formation of a gradient of curing agent concentration, causing a higher degree of crosslinking in the near interfacial regions but leaving a region about 1000 A away from the interface with a reduced curing agent concentration, hence a less than optimum degree of cure.

In some instances, interphase regions are intentionally created to enhance the strength and durability of a composite structure. An example of this is the application of silane coupling agents to adhesive joints, fiber reinforced composites, and coatings formulations.[9] Silane coupling agents are compounds with a high degree of functionality, capable of strong interaction with both the adhesive or coating and substrate. Thin films only a few molecular layers thick seem to give the best improvements in performance. They appear to be capable of improving composite performance by several mechanisms. They can function to improve the mechanical strength of an interface by forming interpenetrating polymer networks with the organic phase[10,11] or by forming primary chemical bonds with the organic phase.[12] Some investigators have also found evidence for the formation of primary chemical bonds between the silane and the inorganic phase.[9] Silanes have also been shown to function as corrosion inhibitors on substrates such as aluminum.[12,13]

Other investigators have used reflection infrared techniques to study the formation and composition of interphases. One study used attenuated total reflectance infrared spectroscopy to investigate curing reactions of epoxy/anhydride mixtures on germanium and silane-treated germanium.[14] It was found that humid aging of the germanium surfaces accelerated the consumption of anhydride in the near interfacial regions during cure, thereby reducing the amount of crosslinking that occurred within a few thousand Angstroms of the interface. Aminosilanes applied to the germanium surface likewise decreased the amount of crosslinking by consuming anhydride, resulting in amide formation between amines in the silane and the anhydride curing agent. This technique has been extended to the study of carbon surfaces as models of carbon fiber composites[15] and it was found that interphase structure could be related to the mechanical properties of the composites.

This paper discusses in some detail the influence of an aluminum oxide surface upon the composition of an epoxy adhesive in contact with the oxide during curing. The presence of the oxide in this instance has resulted in the formation of a distinct interphase region in the adhesive with a structure different from that of the bulk adhesive phase. The primary tools used in this investigation included X-ray photoelectron spectroscopy (XPS) and reflection-absorption infrared spectroscopy (RAIR).

XPS is a highly surface sensitive technique for determining the composition of the uppermost atomic layers of a sample. When the surface of a solid is irradiated with high energy photons (*i.e.*, X-rays), core level electrons can be ejected from elements near the surface if the photon energy is greater than the binding energy of the electron plus the spectrometer work function. Conservation of energy dictates that the kinetic energy of the ejected photoelectrons will be given by

$$T = h\nu - E_b - \phi$$

where

T = kinetic energy of electron

$h\nu$ = incident photon energy

E_b = binding energy of electron

ϕ = spectrometer work function

The binding energies of the photoelectrons are unique for each element, allowing unambiguous element identification. Moreover, alteration of the chemical state of the parent atom through the formation of chemical bonds results in a shift of the binding energy of the electrons and allows (in some cases) compound identification.

One of the most valuable aspects of XPS is the ability to vary the analysis depth from a few Angstroms to a few tens of Angstroms by varying the angle between the sample and the electron energy analyzer. This effect is related to the limited mean free path of photoelectrons in solids. The penetration depth of X-rays in solids is relatively large and, in an XPS experiment, photoelectrons are ejected from the core levels of atoms located quite a great distance from the surface. The probability of these electrons escaping the surface of the material without losing energy to inelastic collisions is low and is a function of the material, the kinetic energy of the electron, and the depth beneath the surface from which the photoelectron originated. The depth below which less than $1/e$ of the ejected photoelectrons of a given energy escape the sample surface without having undergone inelastic collisions is termed the escape depth and represents the depth of material that is responsible for most of the intensity of a photoelectron peak. Decreasing the angle between the sample surface and the electron energy analyzer (known as the spectrometer exit angle) increases the distance that a given photoelectron must travel in the material before escaping the surface, thereby increasing its probability of losing energy to an inelastic collision. This is illustrated in Figure 1. When the sample surface is normal to the analyzer (Figure 1A), the distance which a given photoelectron must travel to escape the material is represented by x, and the effective sampling depth is determined by the mean free path of the electrons. When this angle is decreased (Figure 1B), the distance that a given electron must travel to escape the surface and be detected increases by $1/\sin\theta$, hence at smaller angles the electrons have a longer effective path. Electrons originating from deeper within the sample are therefore more likely to have lost energy to inelastic collisions before escaping the surface. These electrons form part of the background signal of the spectrum.

XPS data obtained from a surface at several exit angles makes it possible to distinguish between several different surface morphologies.[16,17] For a sustrate/overlayer surface structure where

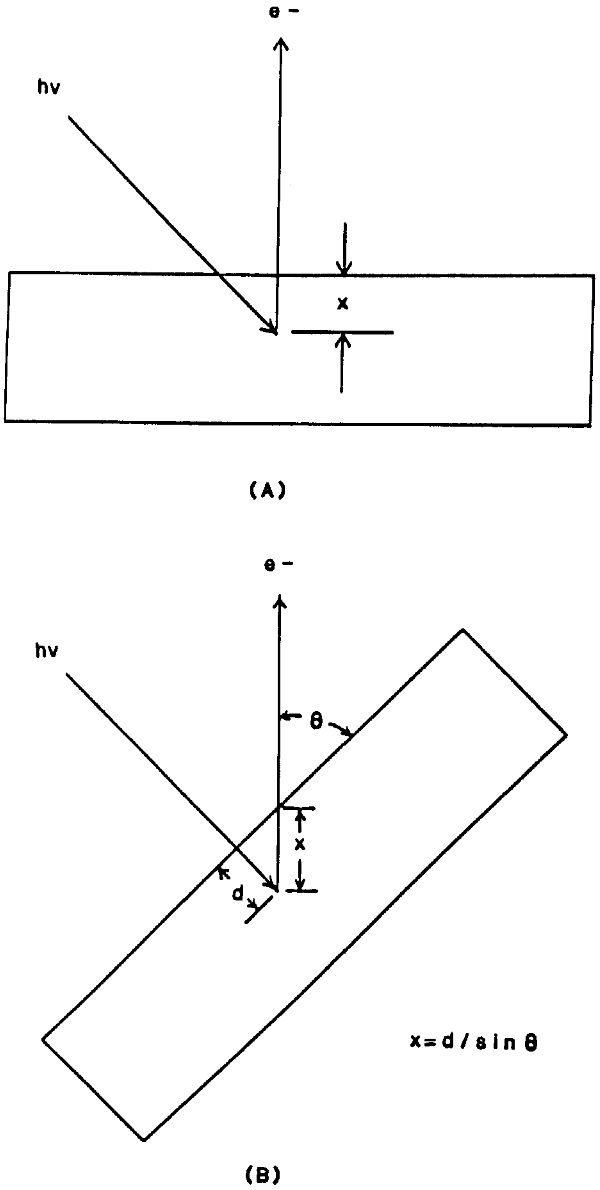

FIGURE 1 Angle-resolved XPS analysis using (A) normal and (B) non-normal exit angles.

the thickness of the overlayer is less than the escape depth of the photoelectrons, the intensity of the signal arising from the substrate species increases exponentially as the angle between the electron energy analyzer and the sample surface is increased. The intensity of signals arising from species in the overlayer decrease in a similar exponential manner as the spectrometer exit angle is increased.

Other surface morphologies can be identified by the functional dependence of intensity on exit angle.[16,17] If the surface phase is present as a discontinuous film whose thickness is less than the electron escape depth then the intensity of the signal arising from the surface phase will again show an exponential dependence on exit angle. However, both substrate and overlayer species will be present at the surface in this instance, and the intensity of peaks arising from species in the bulk or substrate phase will not show a strong dependence on exit angle.

If the surface phase is present as a discontinuous film whose average thickness is greater than the electron escape depth then both phases will again be visible at all exit angles. The relative intensity of peaks arising from material in the surface phase will not, however, show a dependence on spectrometer exit angle.

RAIR is a technique for obtaining the infrared spectra of extremely thin films on reflecting substrates. The method involves reflecting infrared radiation that is polarized parallel to the plane of incidence off of the surface at large, grazing angles of incidence. Under these conditions, the incident and reflected waves combine to form a standing wave that has considerable amplitude at the surface. On fairly good specular reflectors such as polished metals, evaporated metal films, or silicon wafers, the technique allows reasonable spectra to be obtained from absorbing films of approximately monomolecular coverage. Because the desired signal in a typical RAIR experiment is only a small percentage of the total reflected energy, FTIR instruments greatly facilitate the use of this technique by providing improved signal-to-noise ratios and greatly reduced scan time as compared to typical dispersive instruments.

One major problem encountered in the study of interfaces and interphases is obtaining the region of the composite of interest in a physical form that it is possible to study. This is particularly a problem in the study of fiber reinforced composite materials. As a result, investigators frequently resort to modeling the desired interphase in a form more amenable to study. The samples used in this investigation consisted of beams of adhesive cast onto polished aluminum substrates. The geometry of these samples results in large residual stresses forming in the sample during cooling from the elevated temperature cure. Operating in a shear mode, these stresses allow cracks to be easily propagated through the weakest part of the interfacial region. This allows determination of the location and composition of the weakest link in the system by presenting it for analysis.

II. EXPERIMENTAL

Samples were prepared by mechanically polishing beams of 2024-T3 aluminum using metallographic techniques. To insure surfaces with a minimum of contamination, deionized, carbon-filtered water was used during all phases of sample preparation and all handling of the samples was done with clean rubber gloves. The beams were initially degreased in acetone and then washed with detergent, followed by a 5-minute soak in a sulfuric acid-sodium dichromate cleaning solution. The polishing process included dry grinding with succesively finer grades of dry SiC paper followed by wet grinding using 14.5 micron alumina powder on Microcloth (Beuhler, Inc.). Specimens were then polished on Microcloth using MgO as the polishing medium, resulting in surfaces which were bright mirrors.

Previous analysis of such surfaces using RAIR and XPS[16] demonstrated that they consisted of a thin film (*ca.* 40 A) of amorphous Al_2O_3 and some hydroxide, probably pseudoboehmite, that contained both molecular water (water existing as H_2O) as well as water of hydration (water that was part of the hydroxide structure). The amount of hydrocarbon contamination present on the surfaces as determined by XPS and RAIR was quite small. Wettability envelopes constructed for these surfaces showed[18] that they were wettable by mixtures of DGEBA epoxies and tertiary amine salt curing agents.

The adhesive in the present study consisted of Epon 828 (Shell Chemical Co.), a low molecular weight DGEBA epoxy resin, cured with 10 phr (parts per hundred resin by weight) of triethylenetetraamine (TETA, Fisher Scientific Co.). The resin was degassed in a vacuum oven at 50°C and then combined with the curing agent in a beaker using a magnetic stirrer. Heating of the resin before addition of the curing agent facilitated complete mixing and reduced the viscosity, helping to ensure that complete wetting of the substrate was kinetically possible. Attaining equilibrium wetting of oxide surfaces by viscous fluids like epoxy resins can require very long times at room temperature, considerably more time than required for gelation with many curing agents.

An aluminum mold, lined with 1/8″ thick fluorocarbon plates, was clamped around the freshly prepared substrate and filled with the warm adhesive mixture. The samples were then allowed to cure overnight at room temperature, after which they were removed from the mold and postcured at 100°C for one hour. The resulting sample is shown in Figure 2.

After cooling from the postcure, residual stresses in the beams were high enough to cause visible deflection of the aluminum beam substrate. Interfacial cracks frequently started spontaneously, due to the magnitude of the stresses and the absence of mechanical interlocking with the polished surface, and were easily propagated by applying a light restoring force to the beams. Specimens for XPS and RAIR analysis were sectioned from both the adhesive and the adherend using a band saw with care being taken to avoid contamination of the fresh surfaces. Spectra were obtained from fracture surfaces as soon after fracture as possible, usually within minutes. XPS spectra were obtained at four different exit angles to assist in depth profiling.

XPS spectra were obtained using a Physical Electronics Model

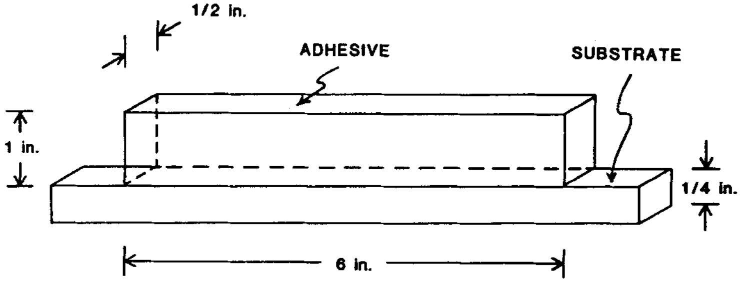

FIGURE 2 Sample geometry for interphase investigations.

5300 spectrometer using MG K_α radiation at a power of 300 watts and a pass energy of 17.9 eV. To correct for sample charging, all binding energies were referenced to the aliphatic C(1s) peak at 284.6 eV.

The curve fitting process that was used to aid in the interpretation of the spectra was based on the techniques outlined in Reference 16. Curve fitting of XPS spectra in the absence of other information about sample composition and chemistry can be a very subjective technique due to the large number of factors that determine the envelope shape. These factors include: i) the percent Gaussian character of the component peaks, ii) peak location, iii) peak width (expressed as full width at half maximum, or FWHM), iv) peak height or intensity, v) number of component peaks that comprise the envelope, and vi) form of the baseline. Without prior knowledge of most of these parameters, or at least close estimates for them, curve fitting is an indeterminate process and obtaining a unique interpretation of a multicomponent spectrum becomes impossible. The curve fitting technique employed in the present study, however, depended only upon the determination of at most 2 unknowns, due to the prior analysis of standards of known composition.

The first of these standards consisted of a sample of polyethylene, which allowed the establishment of the location and shape of the C(1s) peak characteristic of unoxidized hydrocarbons, as well as the characteristic form of the baseline. The % Gaussian character of the peak, primarily a function of the instrument, was also determined through optimization of the curve-fit to this single-component spectrum.

The next sample analyzed was Epon 1007, a higher molecular weight homologue of Epon 828, which is representative of a DGEBA resin in the uncured state. The use of this higher molecular weight resin (which is a solid at room temperature) allowed analysis while avoiding the outgassing in the UHV chamber that might occur with a lower molecular weight liquid resin. This material, like Epon 828, contains only two types of carbon atoms distinguishable by XPS: those bonded to oxygen atoms (both as phenyl ethers and as glycidyl ethers), and those bonded only to other carbon atoms and hydrogen atoms (similar to polyethylene), and therefore allowed an unequivocal establishment of the peak shift expected in the C(1s) spectrum due to the formation of a bond to oxygen. The location of the second, higher binding energy component, due to C—O type species, was determined by constraining its FWHM to that of the main peak (due to C—C type species) which in turn was determined by matching the contour of this component to the right hand side of the envelope. Because the number of components, the % Gaussian character, the baseline shape, and the FWHM were all constrained through a knowledge of the chemistry and through prior analysis of the polyethylene sample, determination of the peak shift and relative intensity of the component due to C—O species was only a matter of several iterations. The relative peak areas of these components in the curve fit of the C(1s) spectrum correlated well to the calculated amounts of C—C and C—O species present, lending credence to the technique.

Finally, a specimen of cured Epon 828/TETA was obtained through the fracture of a block of cured resin and was analyzed to determine the location of the component in the C(1s) envelope due to carbon atoms that are bonded to nitrogen atoms. This spectrum was first fit with the component peaks due to C—O and C—C type species determined through analysis of the neat resin, and then the envelope was completed by the addition of a peak shifted about 1.00 eV to account for the nitrogen atoms present in the curing agent. Again, all of the parameters determining the shape of this component except for intensity and exact shift were constrained to match those of the other two component peaks. As shown in Table I, this procedure resulted in a curve fit that agreed quite well with

TABLE I
Atomic percentages of carbon species found in epoxy adhesive.

	Atomic %			
	C—C	C—N	C—O	C=O
Uncured resin, Calculated	59.0	6.3	35.0	0.0
Cured resin, Calculated	59.0	8.3	33.0	0.0
Bulk resin, Observed	57.0	8.5	32.0	2.0
Interphase, Observed	59.0	11.4	28.0	1.0

the calculated stoichiometry of the system. All subsequent curve fits were constrained to the same parameters determined by analysis of the standards with the exception of peak intensity, which was kept as a variable. The FWHM of all component peaks were constrained to match that of the main C(1s) component peak at 284.6 eV in the individual spectra, as the peak width of the main component was found to shift slightly from spectrum to spectrum.

After long exposure times to heating and X-ray bombardment in the sample chamber of the spectrometer, the envelope shape of the C(1s) peak changed slightly, and curve fits constrained to the peaks determined by analysis of the epoxy standards could not be made to conform to the extreme high binding energy side of the envelope. This necessitated the addition of a small peak (no more than 1 or 2% of the total envelope area) shifted to 2.63 eV higher binding energy from the main C(1s) peak near 284.6 eV. This component is characteristic of carbon atoms with a double bond to oxygen and may indicate auto-oxidation of the resin during prolonged heating under vacuum, as it showed a linear increase in intensity with X-ray exposure time.

The RAIR spectra were obtained using a Perkin-Elmer Model 1800 FTIR equipped with a Harrick Scientific Co. external reflection accessory used at a reflection angle of 78 degrees. Spectra of freshly polished aluminum substrates were subtracted from the spectra of the fracture surfaces to obtain difference spectra of material left on the fracture surfaces.

III. RESULTS AND DISCUSSION

Figure 3 shows the Al(2p) XPS spectrum of the epoxy side of the fracture surface which demonstrates the presence of about 0.5 atomic percent aluminum and indicates that crack propagation occurred at least in part through a region that contained some aluminum oxide. The identity of this peak showed no dependence on the spectrometer exit angle, suggesting two possible structures for the region of fracture, which are shown schematically in Figure 4. One possible structure (Figure 4A) has aluminum oxide present on the epoxy side of the fracture surface not as a continuous film, but rather as islands with thicknesses greater than the escape depth

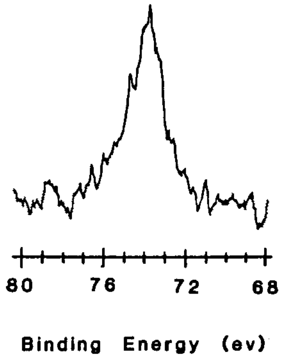

FIGURE 3 Al(2p) XPS spectrum obtained from the adhesive fracture surface.

of the photoelectrons. An alternative possibility (Figure 4B) has a relatively thick region of the adhesive (thick relative to electron escape depth) that contains a small amount of diffused aluminum oxide. Either mode of failure would result in the detection of a weak Al(2p) signal with a relative intensity that was independent of exit angle.

Figure 5 shows the RAIR spectrum of the aluminum side of the

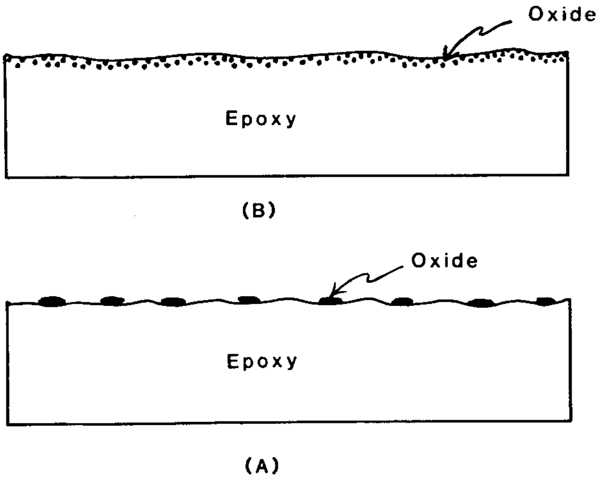

FIGURE 4 Models of adhesive fracture surface showing (A) islands of oxide on the adhesive and (B) interdiffused oxide and adhesive.

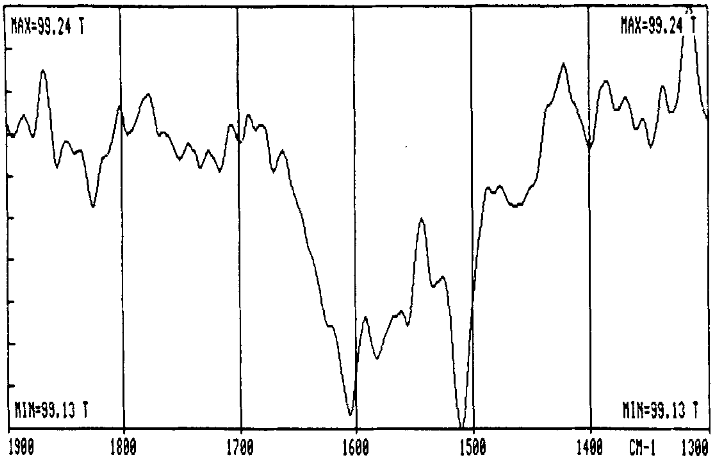

FIGURE 5 Reflection-absorption infrared spectrum obtained from the adherend failure surface.

fracture surface and demonstrates a weak band near 1510 cm^{-1} characteristic of the epoxy resin, indicating that a small amount of resin was retained on the aluminum surface. This information could not be obtained from the C(1s) XPS spectra of these surfaces, which show oxidized hydrocarbons but do not give enough information to allow one to distinguish between the epoxy resin left after the fracture process and the contaminants that were either present on the as-polished surfaces or adsorbed after fracture.

Analysis of the C(1s) XPS spectra of the fracture surfaces gave additional information as to the composition of the region in which failure took place. Figure 6A shows the curve fit of the C(1s) spectrum obtained from a specimen of cured epoxy. This specimen was fractured from the interior of the cured beam and serves as an example of the adhesive cured in the absence of an interface. The main component, located near 284.6 eV, represents electrons originating from carbon atoms that are bonded only to hydrogen atoms or to other carbon atoms. The component shifted to a 1.0 eV higher binding energy from this main peak results from carbon atoms that are bonded to nitrogen atoms, while the component shifted upscale 1.68 eV from the main peak is characteristic of carbon atoms with a single bond to an oxygen atom.

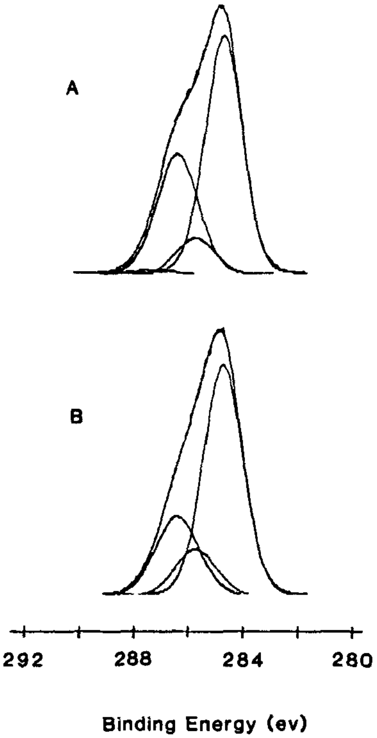

FIGURE 6 C(1s) XPS spectra obtained from (A) bulk cured adhesive and (B) adhesive fracture surface.

Table I shows the percentages of the different types of carbon atoms present in the adhesive/curing agent mixture, calculated for the bulk adhesive/curing agent mixture before and after cure and also from spectra of the bulk cured resin and of the epoxy side of the fracture surface.

The curing reaction between epoxies and aliphatic amines results in the conversion of primary and secondary amines to secondary and tertiary amines as the amines open up the glycidyl ether rings through nucleophilic attack. Each of these crosslinking steps results in the formation of one C—N bond at the expense of one C—O bond. Because of this, as the curing reaction proceeds there is an increase in the percentage of carbon atoms that are bonded to nitrogen atoms and a decrease in the percentage of carbon atoms that are bonded to oxygen atoms.

Table I shows that about 6.3% of the carbon atoms present in the uncured resin/curing agent mixture should exist as C—N species. If the curing reaction proceeds so that all of the primary amines react to form tertiary amines, approximately 8.3% of all of the carbon should exist as C—N type material. The spectrum of the bulk cured resin (Figure 6A) shows that about 8.5% C—N type material is present. This suggests that the reaction between TETA and DGEBA epoxies involves mostly the primary amines of the curing agent.

Figure 6B shows the spectrum obtained from the epoxy side of the fracture surface. As noted in Table 1, the area of the component peak due to C—N type material has increased to about 11.4% of the entire peak area, while the area due to C—O type material has decreased to about 28%. Atomic concentration measurements show, however, that the total amount of nitrogen and oxygen present on the surface is unchanged from the bulk. This suggests that the degree of crosslinking occurring in the interphase region is greater than that occurring in material located a farther distance away from the interface.

Additional information about the chemical composition of the interphase region was obtained from an examination of the N(1s) spectra of both the bulk resin and of the fracture surfaces. Figure 7A shows the N(1s) spectrum obtained from the bulk, cured material. Only one type of nitrogen species is expected in the bulk cured resin, corresponding to nitrogen atoms that are bonded to carbon and hydrogen atoms and found at about 398.0 eV in the absence of sample charging. This spectrum shows a small amount of a higher binding energy material, however. The component shifted to about 1.5 eV higher binding energy from the main peak is characteristic of amine nitrogens that are protonated[19,21,22] (therefore in a higher binding energy state) and this component accounts for about 3.2% of the total envelope area. The origin of this minor component in the bulk, cured resin may be due to the protonation of a small percentage of the amine nitrogens by the hydroxyls present in the cured DGEBA resin. The formation of amine hydrochlorides with residual HCl, a byproduct of the manufacture of DGEBA resins, was considered as a possibility, but was ruled

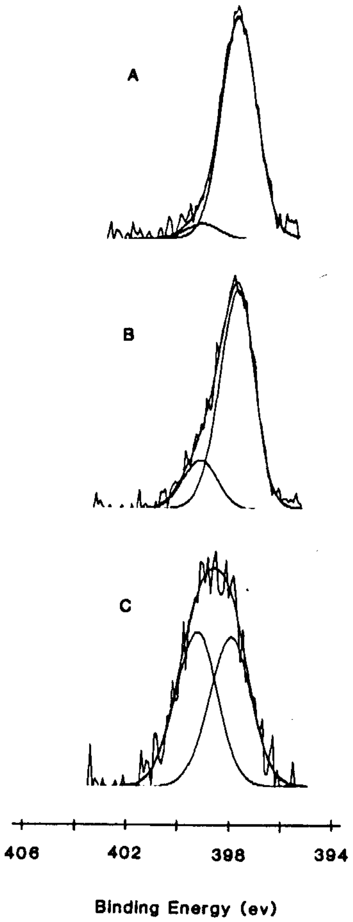

FIGURE 7 N(1s) XPS spectra obtained from the (A) bulk cured adhesive, (B) adhesive fracture surface, and (C) adherend fracture surface.

out because of the absence of any trace of chlorine in spectra of the cured resin. Likewise, the formation of amine carbonates or bicarbonates with dissolved CO_2 was considered, but spectra obtained from cured adhesive prepared in an N_2 atmosphere from carefully degassed resin and curing agent still demonstrated this component.

Figure 7B shows the N(1s) spectrum obtained from the epoxy side of the fracture surface. The higher binding energy component now accounts for about 25% of the entire peak area, suggesting that a higher percentage of the amines present near the surface exist in a higher binding energy state.

Figure 7C shows the N(1s) spectrum obtained from the aluminum side of the fracture surface. In this spectrum, the higher binding energy component accounts for about 50% of the envelope. Approximately half of all of the amines present in the region located within a few atomic layers of the oxide surface exist in a higher binding energy state.

Previous work using RAIR[18] has shown that the oxide present on the surface of mechanically polished 2024-T3 aluminum contains a large amount of hydroxide and molecular water. Isoelectric point measurements of these same surfaces[18,20] indicate that they are slightly acidic, with a pK_a between 7 and 4.5. It is likely that the acidic hydroxyls present on the as-polished surfaces are capable of protonating the amines present in the curing agent, suggesting that the higher binding energy nitrogen material present near the oxide surface primarily represents the protonation of amines by hydroxyls present in the aluminum hydroxide.

Other work has also indicated that these surfaces are able to protonate amines. XPS spectra of thin films of N-propylamine adsorbed onto polished aluminum show the presence of high binding energy N(1s) electrons attributed to protonated amines.[22] Also, angle-resolved XPS of thin films of amine functional silanes deposited onto polished aluminum from dilute solution show high binding energy nitrogen material in the regions close to the oxide, and less high binding energy material farther away from the oxide surface.[22]

As stated earlier, aluminum is present on the epoxy side of the fracture surface and is distributed vertically within a region that is thicker than the escape depth of the Al(2p) electrons. This conclusion is based on the lack of dependence of the Al(2p) peak intensity on exit angle. The high binding energy nitrogen material found on the epoxy side of the fracture surface, ascribed to protonated amino groups, similarly does not show an angle dependence, indicating that it is also distributed vertically throughout a region extending farther than the electron escape depth. The demonstrated ability of the oxide to protonate these amines suggests that the protonated amine compounds present on the adhesive side near the interface may be associated with the aluminum oxide that either fractured from the adherend surface during crack propagation or diffused into this region from the adherend surface during manufacture.

Only a very small amount of adhesive was left of the adherend side of the sample after fracture. Because of this, most of the amines present on the aluminum side of the fracture surface are in a region extremely close to the oxide surface, explaining why a larger percentage of the amines in this region are protonated.

Primary and secondary aliphatic amines act as initiators in the polymerization of epoxy resins. The amine nitrogen attaches to the terminal carbon atom of the epoxy ring in a nucleophilic addition reaction, opening the epoxy ring and forming an oxygen anion from the glycidyl oxygen. Chain propagation occurs as these oxygen anions open other epoxy rings through nucleophilic addition. Both the initiation step as well as the chain propagation steps require the presence of a proton donor to stabilize these intermediate oxygen anions.[23,24]

The concentration of these proton donors is known to be a rate-controlling factor in the curing reaction.[24] The concentration of material capable of functioning in this proton-donating role is low in the bulk resin and limited to the alcohol groups that are part of higher molecular weight DGEBA molecules and possibly to other stray molecules such as water or other impurities.

Proton donators are abundant, however, near the hydroxyl-rich aluminum oxide surface. This is suggested by the presence of protonated amino nitrogens in the vicinity of the aluminum oxide. These same hydroxyls are probably capable of catalyzing the curing reaction and are, therefore, probably responsible for the large amount of chain initiation steps detected in these same regions. As a result, the average molecular weight and crosslink density of the cured epoxy in this interphase region is probably considerably different from that of the bulk material.

IV. CONCLUSIONS

It has long been recognized that the chemical environment near the substrate surface in a composite structure is different from that found in the bulk organic phase. It is therefore reasonable to assume that proximity to this surface should be sufficient to alter the composition and properties of the organic phase in its vicinity. This has generally been difficult to demonstrate, however, for several reasons. The differences in structure and composition in this region may be subtle and, therefore, difficult to detect. Moreover, the region to which these changes are restricted may be comprised of only a few molecular layers, requiring analysis techniques that are extremely surface sensitive.

X-ray photoelectron spectroscopy and reflection-absorption infrared spectroscopy, combined with a sample of suitable geometry, has allowed the detection and analysis of this interphase region in an aluminum-epoxy adhesive joint. In this system, the aliphatic amine curing agent appears to be partially protonated by the surface hydroxide. Moreover, the epoxy adhesive has a very different network structure in the regions near the oxide surface, probably due to the ability of the hydroxyls present on the oxide to catalyze the curing reaction.

The specimen geometry used in this study was such that the cracks were propagated by a combination of shear stresses (arising from cure shrinkage and predominantly parallel to the long axis of the specimen), and normal stresses (resulting from application of the three-point bend that initiated failure). This type of mixed mode stress distribution results in crack propagation very close to the interface. The distance away from the interface in which crack propagation occurs probably depends upon the plastic zone radius of the crack tip[25] and is typically within 1000 Angstroms of the substrate surface.

Because mixed mode loading directs crack propagation into the near interfacial regions, adhesive joint strength will be very sensitive to the mechanical and chemical properties of the adhesive in this region. An adherend surface which results in the formation of overcured (hence brittle) adhesive near the interface will therefore tend to be weaker in the region where the structure is most sensitive.

V. Acknowledgements

This work was supported in part by a grant from the Office of Naval Research. The X-ray photoelectron spectrometer was obtained through grants from the Department of Defense, Armco, Inc., and Republic Steel Corporation. The Fourier transform infrared spectrophotometer was obtained through a grant from the Perkin-Elmer Corporation. The assistance of Kristen A. Boerio in the preparation of the figures is gratefully acknowledged.

VI. References

1. J. D. Venables, *et al.*, *Appl. Surf. Sci.* **3,** 88 (1979).
2. D. I. Packham, in *Adhesion Aspects of Polymeric Coatings,* K. L. Mittal, ed. (Plenum Press, N.Y., 1985).
3. J. D. Venables, *J. Matls. Sci.* **19,** 2431 (1984).
4. L. H. Sharpe, *J. Adhesion* **4,** 51 (1972).
5. L. T. Drzal, in *Advances in Polymer Science,* Vol. 75, K. Dusek, Ed. (Springer-Verlag, N. Y., 1986).
6. L. P. Buchwalter and J. Greenblatt, *J. Adhesion* **19,** 257 (1986).
7. C. M. Chan, *ibid.*, **15,** 217 (1983).
8. J. L. Racich and J. A. Koutsky, in *Chemistry and Properties of Crosslinked Polymers,* S. S. Labana, Ed. (Academic Press, N.Y., 1977), p. 303.
9. E. P. Pleuddemann, *Silane Coupling Agents,* (Plenum Press, N.Y., 1982).
10. N. H. Sung, A. Kaul, I. Chin, and C. S. P. Sung, *Poly. Eng. Sci.* **22,** 637 (1982).
11. E. P. Pluedemann and G. L. Stark, *Proc. 35th Ann. Tech. Conf.*, SPI Reinforced Plastics/Comp. Inst., Sec. 20-B, 1980.
12. F. J. Boerio, R. G. Dillingham and R. C. Bozian, *Proc. 39th Ann. Tech. Conf.*, SPI Reinforced Plastics/Comp. Inst., Sec. 1-A, 1984.
13. F. J. Boerio and C. H. Ho, *J. Adhesion* **21,** 25 (1987).
14. A. Garton, *J. Polym. Sci., Polym. Chem. Ed.* **22,** 1495 (1984).
15. A. Garton, private communication, 1986.
16. A. Dilks, in *Electron Spectroscopy: Theory, Techniques and Applications,* Vol. 4, C. R. Brundle and A. D. Baker, Eds. (Academic Press, N.Y., 1981).
17. H. P. Thomas and J. M. O'Malley, *Macromolecules* **12,** 323 (1979).
18. R. G. Dillingham, D. J. Ondrus, and F. J. Boerio, *J. Adhesion* **21,** 95 (1987).
19. P. R. Moses, *et al.*, *Anal. Chem.* **50,** 576 (1978).
20. G. A. Parks, *Chem. Rev.* **65,** 177 (1965).
21. F. J. Boerio, unpublished data.
22. R. G. Dillingham, unpublished data.
23. *Handbook of Epoxy Resins,* H. Lee and K. Neville, Eds. (McGraw-Hill, N.Y., 1967).
24. B. A. Rozenburg, in *Advances in Polymer Science,* Vol. 75, K. Dusek, Ed. (Springer-Verlag, 1986).
25. W. D. Bascom, C. O. Timmons, and R. L. Jones, *J. Mat. Sci.* **10,** 1037 (1975).